

Thermodynamics of Si etching and removal of the oxide layer from Si cluster surface using KOH solution: A DFT study

Mudar Ahmed Abdulsattar^{1*}, Saad Mahdi Salih¹, Ahmed Abdulsattar Almaroof², Adeebah Muhammedsaed Alhilaly², Maad Ahmed Almaroof²

¹ Ministry of Science and Technology, Baghdad, Iraq. ² Ministry of Education, Baghdad, Iraq.

Correspondence: Mudar Ahmed Abdulsattar, Ministry of Science and Technology, Baghdad, Iraq. Email: mudarahmed3@yahoo.com

ABSTRACT

The oxide layer on the Si surface needs to be removed in addition to the removal of Si upper layers before many industrial manufacturing processes. Thermodynamics of removal of these layers by KOH solution is described using density functional theory including Gibbs free energy, enthalpy, and entropy. Results show that the degree of oxidation is the most effective factor in determining the possibility and speed of removal. Small SiO₂ spots on the Si substrate can be removed with mild speed. Thick SiO₂ layers are the most difficult and time-consuming layers to remove using a KOH solution. The removal of thin oxide layers on the Si surface is performed by the direct reaction of KOH molecules. Thick oxide layers are removed by the reaction of K⁺ and OH⁻ ions in slower reaction rates due to the hydration of these ions. The calculated thermodynamic quantities of oxidation and removal are in good agreement with experimental findings.

Keywords: Si; Etching; Density functional theory

Introduction

Silicon ^[1, 2] is a critical semiconductor in the manufacturing of many electronic devices ^[3, 4], solar cells, computers, etc. Many of these manufacturing processes include the removal of the surface oxide layer that usually acts as a contact insulator. The removal process includes either alkali agents such as potassium hydroxide (KOH) or acids such as hydrogen fluoride (HF) ^[5]. Due to the toxicity of HF ^[6], the use of HF is less desirable with respect to the less toxic KOH. However, the use of KOH encounters some difficulties especially when the oxide layer is thick (several nanometers). The process of using KOH to wet etching Si surface can be managed to produce a surface with low roughness and high

surface quality ^[7, 8]. This method of etching also enhances the mechanical properties of Si ^[9]. The etching rate can be increased using additives such as alcohol ^[10]. The temperature at which the etching is preferable is at 80°C or near the boiling point of the KOH solution ^[11].

Thermodynamic simulation using density functional theory of many chemical reactions proved to produce further information and illustrations that complete our understanding of the reaction process ^[12, 13]. The simulation can predict approximate temperatures in which the reaction peak or minima is desired. Quantities such as the change in Gibbs free energy, enthalpy or entropy is of vital importance to determine whether the reaction will proceed or not, the heat of reaction, and the order-disorder direction of the reaction.

In the present work, we investigated theoretically the removal of silicon and silicon oxide layers from the surface of the silicon cluster shown in Fig (1). Depending on the kind and thickness of the silicon oxide layer, several reactions were investigated including the reaction of molecules or ions. A comparison with the experiment was performed whenever such experimental data was available.

Access this article online

Website: www.japer.in

E-ISSN: 2249-3379

How to cite this article: Mudar Ahmed Abdulsattar, Saad Mahdi Salih, Ahmed Abdulsattar Almaroof, Adeebah Muhammedsaed Alhilaly, Maad Ahmed Almaroof. Thermodynamics of Si etching and removal of the oxide layer from Si cluster surface using KOH solution: A DFT study. J Adv Pharm Educ Res. 2020;10(2):77-83.
Source of Support: Nil, Conflict of Interest: None declared.

This is an open access journal, and articles are distributed under the terms of the Creative Commons Attribution-Non Commercial-ShareAlike 4.0 License, which allows others to remix, tweak, and build upon the work non-commercially, as long as appropriate credit is given and the new creations are licensed under the identical terms.

Theory

In the present work, we used B3LYP (Becke, three-parameter, Lee-Yang-Parr) density functional theory (DFT) combined with 6-311G** basis functions that are suitable in terms of accuracy and time and computer resource consumption^[14]. Si₁₄ cluster in Fig (1a) was used to simulate the unoxidized silicon surface. This cluster was suitable since oxygen molecules and atoms experience the same effect within the bulk silicon surface including three to four neighboring atoms. Mainly three kinds of oxides can occur on the surface of this cluster. If only one bond from the two bonds that connect the two oxygen atoms in the oxygen molecule is broken, then oxygen (bridge) is formed on

the surface of the silicon cluster as in Fig (1b). If the two bonds of the oxygen molecule are broken, then the silicon oxide will look like that in Fig (1c) that we shall refer to as (surface) oxidation. Repeating the last oxidation process (surface oxidation) several times, a piece of silicon dioxide (SiO₂) will be created as in Fig (1d) which we shall refer to as (complete) oxidation. Other reaction reactants and products such as O₂, H₂, H₂O, K₂SiO₃ or ions such as K⁺ and OH⁻ are simpler to represent using our above theory since they are either in the gas or aqueous phase. Gaussian 09 suite of programs was used to perform present calculations^[15]. A complete discussion of the relevant equations was used in the Gaussian 09 program to calculate thermodynamic quantities given in the Gaussian 09 report^[16].

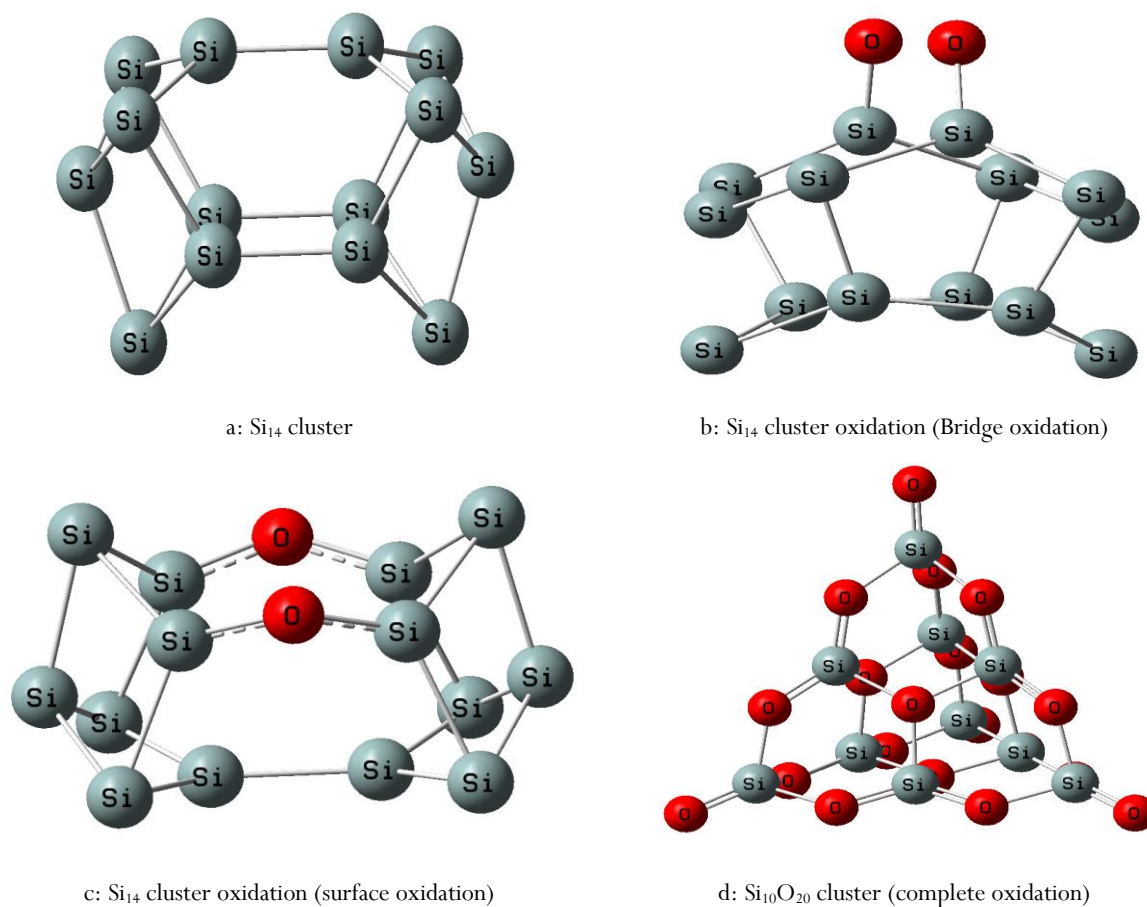


Figure 1: Degrees and steps of Si cluster oxidation. Molecules are shown with optimized structures.

Results and discussion

The reaction of oxygen with the Si cluster can be viewed as a three-step reaction as we discussed above. The first step is the formation of the oxygen bridge (breaking one bond between oxygen atoms) on the Si cluster surface as shown in Fig (1b) and the second step is the surface oxidizing reaction (breaking the two bonds between oxygen atoms) as shown in Fig (1c). Thermodynamic quantities of these reactions are shown in Table 1 (reactions 1 and 2) at 25°C and 1 atmosphere. Gibbs free energy of these two reactions was -4.509 and -8.028 eV for the

bridge and surface oxidation reactions respectively. The temperature variation of these two reactions (0-100 °C) is shown in Fig (2). This figure shows that a small change of the above energies occurs as we increase the temperature. As the oxidation process proceeds, a layer of silicon dioxide is formed similarly to that of Fig (1d) that can be described by reaction number 3 in Table 1. Reaction number 3 in Table (1) is normalized to the reaction of one silicon atom with one oxygen molecule to be compatible with reactions 1 and 2. The value of Gibbs free energy of this reaction is -8.65 eV which will proceed depending on the ability of O₂ molecules to diffuse through silicon lattice.

Table 1: Thermodynamic quantities of considered reactions at 25°C and 1 atmosphere are shown that include change in Gibbs free energy (ΔG), enthalpy (ΔH), and entropy (ΔS).

Reaction	ΔG (eV)	ΔH (eV)	$\Delta S \times 10^{-3}$ (eV/K)
1 $\text{Si}_{14} + \text{O}_2 \rightarrow \text{Si}_{14}\text{O}_2$ (Bridge)	-4.509	-4.912	-1.350
2 $\text{Si}_{14} + \text{O}_2 \rightarrow \text{Si}_{14}\text{O}_2$ (Surface)	-8.028	-8.394	-1.229
3 $\frac{1}{10} \text{Si}_{10} + \text{O}_2 \rightarrow \frac{1}{10} \text{Si}_{10}\text{O}_{20}$ (Complete)	-8.650	-9.193	-1.821
4 $2\text{KOH} + \text{Si}_{14}\text{O}_2$ (Bridge) $\rightarrow \text{K}_2\text{SiO}_3 + \text{H}_2\text{O} + \text{Si}_{13}$	-2.163	-1.767	1.327
5 $2\text{KOH} + \text{Si}_{14}\text{O}_2$ (Surface) $\rightarrow \text{K}_2\text{SiO}_3 + \text{H}_2\text{O} + \text{Si}_{13}$	1.356	1.7154	1.206
6 $2\text{KOH} + \text{Si}_{13} + \text{H}_2\text{O} \rightarrow \text{Si}_{12} + \text{K}_2\text{SiO}_3 + 2\text{H}_2$	-0.183	-0.094	0.3
7 $2\text{KOH} + \text{Si}_{10}\text{O}_{20}$ (Complete) $\rightarrow \text{K}_2\text{SiO}_3 + \text{H}_2\text{O} + \text{Si}_9\text{O}_{18}$	5.768	6.176	1.366
8 $\text{KOH} \rightleftharpoons \text{K}^+ + \text{OH}^-$	6.895	7.3	1.356
9 $2\text{K}^+ + 2\text{OH}^- + \text{Si}_{14}\text{O}_2$ (Bridge) $\rightarrow \text{K}_2\text{SiO}_3 + \text{H}_2\text{O} + \text{Si}_{13}$	-15.953	-16.366	-1.386
10 $2\text{K}^+ + 2\text{OH}^- + \text{Si}_{14}\text{O}_2$ (Surface) $\rightarrow \text{K}_2\text{SiO}_3 + \text{H}_2\text{O} + \text{Si}_{13}$	-12.435	-12.884	-1.506
11 $2\text{K}^+ + 2\text{OH}^- + \text{Si}_{13} + \text{H}_2\text{O} \rightarrow \text{Si}_{12} + \text{K}_2\text{SiO}_3 + 2\text{H}_2$	-14.033	-14.693	-2.413
12 $2\text{K}^+ + 2\text{OH}^- + \text{Si}_{10}\text{O}_{20}$ (Complete) $\rightarrow \text{K}_2\text{SiO}_3 + \text{H}_2\text{O} + \text{Si}_9\text{O}_{18}$	-8.022	-8.423	-1.346

When KOH molecule reacts with the surface of oxidized silicon cluster, the bridge oxide removal reaction proceeds according to its Gibbs free energy value -2.163 eV (Table 1 reaction 4), however, the removal of the surface oxidation reaction is halted due to its positive value 1.356 eV (Table 1 reaction 5). After the removal of the oxide layer in the bridge case, the removal of Si atoms from the Si cluster proceeds as in reaction 6 of Table 1. The removal of the complete oxide layer is halted and is described by reaction 7 of Table (1). The Gibbs free energy of this reaction is 5.768 eV. Fig (3) shows Gibbs free energy of Si surface etching and oxidation removal by KOH as a function of temperature including bridge, surface, and complete oxidation. As a strong base, KOH partially dissociates in its aqueous solution as in Table (1) reaction 8. The degree of dissociation depends on temperature, concentration, and dissociation constant in addition to other factors. The dissociated ion fragments of KOH (K^+ and OH^-) reacts with surrounding water molecules creating solvation shell around each ion [17-20] as in Fig (4) for the K^+ ion. On the other hand, the reaction of the ions with silicon surface oxide gains the extra dissociation reaction energy (6.895 eV) as in reactions 9-12 in Table (1). Although these reactions with the ions are now energetically favorable, their reaction rates are very weak because of the hydration shell that creates dragging force on the ions. The complete neutral KOH molecule has a smaller hydration shell, and as a result, KOH molecule reaction rates are an order of magnitude faster than their ions. Experimentally, the reaction rates of reactions that are favorable with KOH molecules are in the order of microns/hour while reactions that are favorable only with ions are in the order of nm/hour [21, 22]. Fig (5) shows Gibbs free energy of Si etching and surface oxidation removal by K^+ and OH^- ions as a function of temperature including bridge, surface, and complete oxidation. Enthalpies of reactions are calculated in Table (1) to show the amount of heat released or absorbed in each reaction. Oxidation reactions are exothermic reactions which are also the case of ionic reactions as in Table (1). KOH reactions are endothermic

reactions except for oxide bridge and most Si etching reaction range (2-93 °C). The entropy of etching, oxidation and oxide removal discriminate order-disorder reactions. All KOH molecule reactions have positive entropy values (disorder reactions) while oxidation reactions and K^+ and OH^- ions reactions have negative entropy values (order reactions) as in Table (1). To check the correctness of our thermodynamic calculations, we can use SiO_2 experimental formation energies which are well-tabulated quantities [23]. The SiO_2 experimental Gibbs free energy, enthalpy and entropy formation energies are -8.876 eV, -9.439 eV, -1.888×10^{-3} eV/K respectively [23]. These values can be compared with our calculated values for bridge oxidation, surface oxidation and complete oxidation of Table (1) (reactions 1, 2 and 3 respectively). Good agreement can be seen with the complete oxidation. All Gibbs free energy, enthalpy, and entropy values gradually increase towards the experimental values mentioned above except surface oxidation entropy in reaction 2 in Table (1). This can be interpreted by the disorder that is formed when the two oxygen atoms entered the Si surface. However, when all the silicon atoms are oxidized, a kind of order is formed that decreases the value of entropy (negative value) towards its value in the complete oxidation reaction 3. The number of ions and the reactivity of materials increase with temperature. As can be interpolated from Fig (3), the temperatures of negative Gibbs free energy of Si etching reaction are in the range of 2-93 °C which includes the experimentally preferred temperature for silicon etching at 80 °C [24-26]. Usually, when we conduct a reaction at higher temperatures, a higher number of collisions between particles take place as described by collision theory. This explains why higher temperatures in the range of negative Gibbs energy is preferred. References [12-16, 27] give a suitable description of the equations that are involved in the present calculations. Thick layers of SiO_2 may be removed from the Si surface using heated KOH but with a slow rate compared with Si removal. The Si etching rate depends on the kind of Si surface exposed to

KOH. The rate of SiO₂ removal is in the range of 300 nm/hour for a 30% KOH solution at 80 °C. HF can also remove native silicon oxide. However, HF toxicity can reach fatal levels if not used with precautions. KOH can irritate skin or eyes, but it is nontoxic and rarely reaches fatal levels. Experimentally, KOH can etch Si surface roughly if used with concentrations less than

30%. Small concentrations of KOH are not quantitatively adequate to remove both Si and its oxide. The high rate of Si etching in concentrated KOH will remove Si and its oxide in a competing speed and reduces roughness by moving around the SiO₂ layer by removing Si.

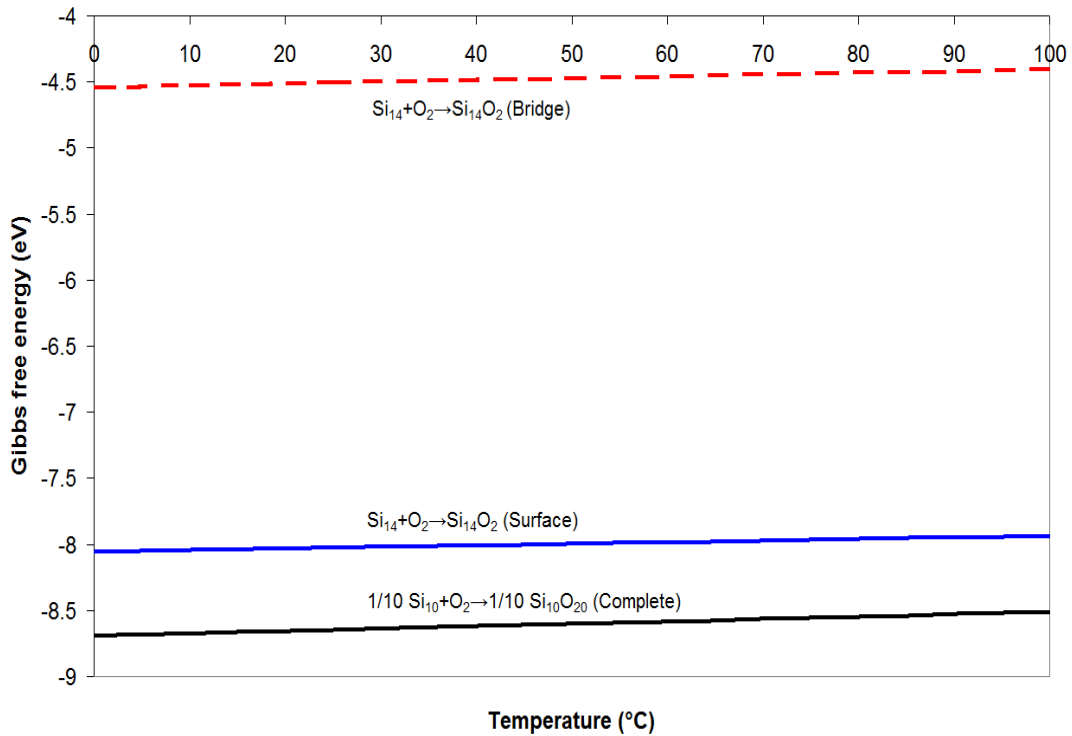


Figure 2: Gibbs free energy of Si surface oxidation as a function of temperature. Bridge, surface, and complete oxidation energies.

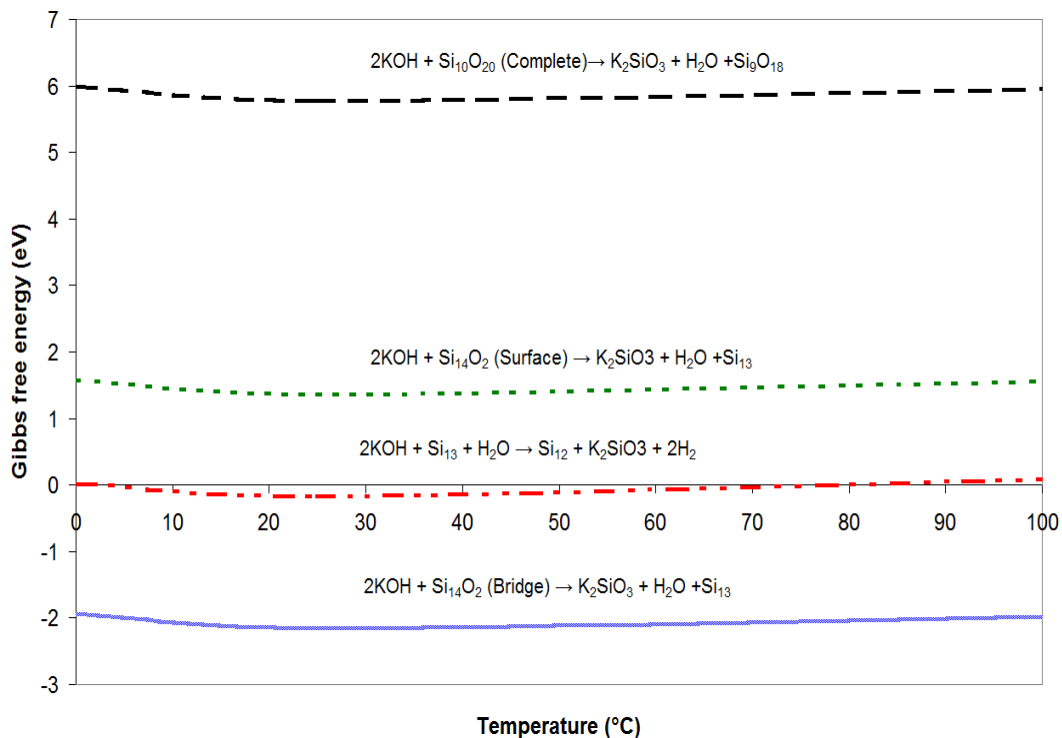


Figure 3: Gibbs free energy of Si surface etching and oxidation removal by KOH as a function of temperature including bridge, surface, and complete oxidation removal.

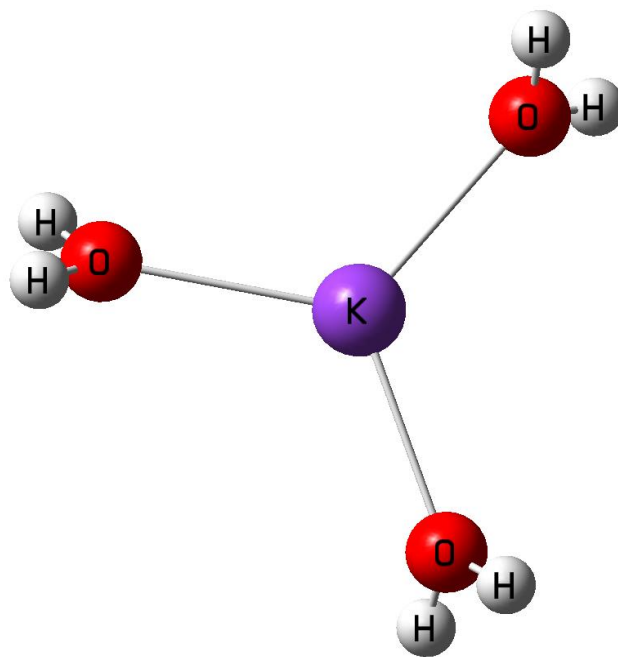


Figure 4: Three water molecules connected to K^+ ion.

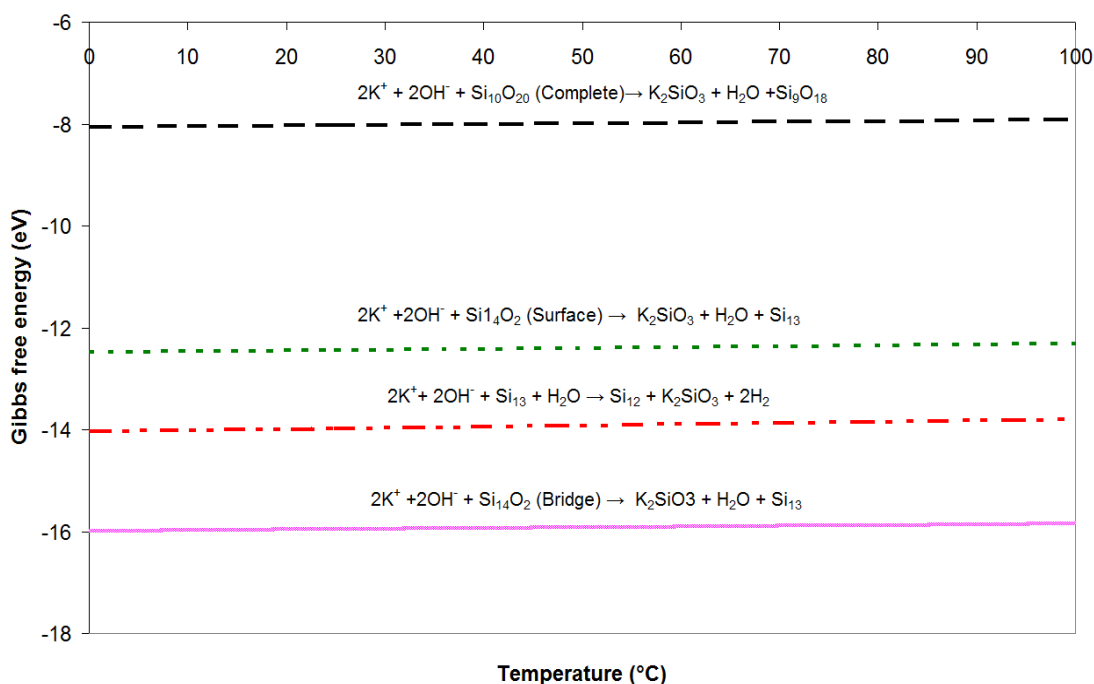


Figure 5: Gibbs free energy of Si surface etching and oxidation removal by K^+ and OH^- ions as a function of temperature including bridge, surface, and complete oxidation removal.

Conclusions

Si etching and removal of oxide layer using KOH solution are described thermodynamically in the present work. Calculations of Gibbs free energy of reactions show that KOH molecule reactions are halted for the removal of Si oxides but can remove surface Si atoms and surface bridged O_2 molecules. The removal of oxides is only possible by the reactions of K^+ and OH^- ions. Due to hydration, K^+ and OH^- ions reactions are orders of

magnitude lower than KOH reaction rates. Enthalpies of reactions are also calculated to show the amount of heat produced or absorbed in each reaction. The entropy of etching, oxidation and oxide removal discriminate order-disorder reactions. All KOH molecule reactions have positive entropy values (disorder reactions) while oxidation reactions and K^+ and OH^- ions reactions have negative entropy values (order reactions). Good agreement of calculated thermodynamic quantities with experimental findings is found.

References

1. Abbasi M, Hashemizadeh S A. Simulation of a GAN-based optical diode with sapphire sub-layer which is Shaped patterned hemisphere, Using Poynting vector analysis. *Pharmacophores*. 2018; 9(3): 48-55.
2. Bizhan Zadeh Sh, Daghighi M, Torkian L. Preparation, Characterization, Equilibrium Isotherms, and Adsorption Kinetics of Al₂O₃-SiO₂ Nanoparticle for Rapid and High Adsorption of Pb(II) From Water. *Int. J. Pharm. Phytopharm. Res*. 2019; 9(1): 51-57.
3. Jafar M, Alshaer F I, Adrees F A. Cyclodextrin Ternary Inclusion Complexation: A Strategy to Improve Solubility of Poorly Soluble Drugs. *Int. J. Pharm. Phytopharm. Res*. 2018; 8(6): 8-17.
4. Singh A, Gaurav K. Advancement in Catalysts for Transesterification in the Production of Biodiesel: A Review. *J. Biochem. Tech*. 2018; 9(1): 17-27.
5. Lu, X., Koppes, M., Bronsveld, P. C. P. Simplified surface cleaning for fabrication of silicon heterojunction solar cells. Paper presented at the AIP Conference Proceedings, 1999 doi:10.1063/1.5049295
6. Sun, R., Nishikawa, T., Nakajima, A., Watanabe, T., Hashimoto, K. TiO₂/polymer composite materials with reduced generation of toxic chemicals during and after combustion - effect of HF-treated TiO₂. *Polym. Degrad. Stab.*, 2002; 78(3), 479-484.
7. Jiao, Q., Tan, X., Zhu, J., Feng, S., Gao, J. Effects of ultrasonic agitation and surfactant additive on surface roughness of Si (1 1 1) crystal plane in alkaline KOH solution. *Ultrason. Sonochem.*, 2016; 31, 222-226.
8. An, S., Lee, S. G., Park, S. -, Lee, E. -, Beom-Hoan, O. Efficacy of low etch rate in achieving nanometer-scale smoothness of Si (1 0 0) and (1 1 0) plane surfaces using KOH and KOH/IPA solutions for optical mold applications. *Sens. Actuators, A*, 2014; 209, 124-132.
9. Shikida, M., Niimi, Y., Hasegawa, T., Sugino, T., Hamaoka, S., Fukuzawa, K. Mechanical strengthening of Si cantilever by chemical KOH etching and its surface analysis by TEM and AFM. *Microsyst. Technol.*, 2014; 21(3), 661-668.
10. Al-Thani, H. A., Al-Jaedi, A. M., Al-Shaibani, S. A., Al-Yafeai, A. A., Hasoon, F. S. The influence of texturing bath conditions on the morphology and optical properties of crystalline silicon. Paper presented at the 2017 IEEE 44th Photovoltaic Specialist Conference, PVSC 2018; 2017, 1-6.
11. Tanaka, H., Yamashita, S., Abe, Y., Shikida, M., Sato, K. Fast wet anisotropic etching of Si {100} and {110} with a smooth surface in ultra-high temperature KOH solutions. Paper presented at the TRANSDUCERS 2003 - 12th International Conference on Solid-State Sensors, Actuators and Microsystems, Dig. Tech. Pap., 2003; 2: 1675-1678.
12. Abdulsattar, M. A. Chlorine gas reaction with ZnO wurtzoid nanocrystals as a function of temperature: A DFT study. *J. Mol. Model.*, 2017; 23(4): 25.
13. Abdulsattar, M. A., Almaroof, H. M. Adsorption of H₂ and O₂ gases on ZnO wurtzoid nanocrystals: A DFT study. *Surf. Rev. Lett.*, 2017; 24, 1850008.
14. NIST Computational chemistry comparison and benchmark database, release 15b, 2011. <http://cccbdb.nist.gov/> (accessed Oct 1, 2018).
15. Gaussian 09, Revision E.01, M. J. Frisch, G. W. Trucks, H. B. Schlegel, G. E. Scuseria, M. A. Robb, J. R. Cheeseman, G. Scalmani, V. Barone, B. Mennucci, G. A. Petersson, H. Nakatsuji, M. Caricato, X. Li, H. P. Hratchian, A. F. Izmaylov, J. Bloino, G. Zheng, J. L. Sonnenberg, M. Hada, M. Ehara, K. Toyota, R. Fukuda, J. Hasegawa, M. Ishida, T. Nakajima, Y. Honda, O. Kitao, H. Nakai, T. Vreven, J. A. Montgomery, Jr., J. E. Peralta, F. Ogliaro, M. Bearpark, J. J. Heyd, E. Brothers, K. N. Kudin, V. N. Staroverov, R. Kobayashi, J. Normand, K. Raghavachari, A. Rendell, J. C. Burant, S. S. Iyengar, J. Tomasi, M. Cossi, N. Rega, J. M. Millam, M. Klene, J. E. Knox, J. B. Cross, V. Bakken, C. Adamo, J. Jaramillo, R. Gomperts, R. E. Stratmann, O. Yazyev, A. J. Austin, R. Cammi, C. Pomelli, J. W. Ochterski, R. L. Martin, K. Morokuma, V. G. Zakrzewski, G. A. Voth, P. Salvador, J. J. Dannenberg, S. Dapprich, A. D. Daniels, Ö. Farkas, J. B. Foresman, J. V. Ortiz, J. Cioslowski, and D. J. Fox, Gaussian, Inc., Wallingford CT, 2009.
16. Joseph W. Ochterski, *Thermochemistry in Gaussian*, <http://gaussian.com/thermo/> (Accessed: 20- October-2018).
17. Mähler, J., Persson, I. A study of the hydration of the alkali metal ions in aqueous solution. *Inorg. Chem.*, 2012; 51(1), 425-438.
18. Izonfuo, W. L., Malinowski, E. R. Hydration numbers of potassium and sodium ions in aqueous-organic solvents. *Discovery and Innovation*, 1997; 9(1-2), 19-23.
19. Meek, K. M., Nykaza, J. R., Elabd, Y. A. Alkaline chemical stability and ion transport in polymerized ionic liquids with various backbones and cations. *Macromol.*, 2016; 49(9), 3382-3394.
20. Masimov, E. A., Abbasov, H. F. Hydration numbers of ions in aqueous solutions of KOH, KCl, KI, and KIO₃ according to refractometric data. *Russ. J. Phys. Chem. A*, 2013; 87(8), 1430-1432.
21. KOH Etching, BYU cleanroom, <https://cleanroom.byu.edu/KOH>, (accessed Oct 1, 2018).
22. Seidel, H., Csepregi, L., Heuberger, A., Baumgörtel, H. Anisotropic etching of crystalline silicon in alkaline solutions: I. orientation dependence and behavior of passivation layers. *J. Electrochem. Soc.*, 1990; 137(11), 3612-3626.
23. Lange, N. A. *Lange's Handbook of Chemistry*, 15th ed. McGraw-Hill New York, 1999.

24. Basu, P. K., Sreejith, K. P., Yadav, T. S., Kottanthariyil, A., Sharma, A. K. Novel low-cost alkaline texturing process for diamond-wire-sawn industrial monocrystalline silicon wafers. *Sol. Energy Mater. Sol. Cells*, 2018; 185, 406-414.
25. Lee, H. Y., Noh, J., Kwak, M. S., Lim, K., Ahn, H. S., Ahn, J., Ryu, J. Fabrication of microholes in silicon wafers by using wet-chemical etching. *New Phys. Sae Mulli*, 2018; 68(8), 834-838.
26. Hajjiah, A. T., Zachariah, S. K., Ghannam, M. Y. Study of surface morphology and optical characterization of crystalline and multi-crystalline silicon surface textured in highly diluted alkaline solutions. *J. Eng. Res.*, 2014; 2(2), 139-153.
27. Abdulsattar, M. A., Resne, A. L., Abdullah, S., Mohammed, R. J., Alared, N. K., Naser, E. H. Chlorine gas sensing of SnO₂ nanoclusters as a function of temperature: A DFT study. *Surf. Rev. Lett.* 2018; 26(4): 1850172 doi:10.1142/S0218625X1850172X.